the first hour, followed by a more gradual increase in saturation magnetization. The transition is more abrupt than might be expected on the basis of a simple exponential decrease; we do not fully understand the physical reasons for this sudden change in rate. As noted earlier, TCRM at 400°C also increased rapidly, then tailed off abruptly. Day *et al.* (*10*) have postulated two stages in the oxidation of a titanomagnetite: (i) the conversion of octahedral Fe^{2+} to Fe^{3+}, followed by (ii) the migration of Ti^{4+} from the spinel lattice to the rhombohedral ilmeno-hematite phases, which results in a more iron-rich magnetite phase. Perhaps these two successive steps are being reflected in our heating experiments.

One of the primary assumptions inherent in any paleointensity study of a rock is that the TRM developed in the laboratory is being compared with a TRM acquired in nature at the time the rock cooled through the Curie temperature (*11*). However, if the original remanent magnetization was induced at temperatures below the final Curie temperature by the oxidation process outlined here, then serious questions are raised as to the validity of Thellier's method.

Our primary conclusion is that for the basalt we studied the remanence is proportional to the field intensity, whether it is simple TRM or whether it is wholly or partially TCRM. On the assumption that the New Mexico basalt is not magnetically unique (and there seems little reason to suspect that it is), we further tentatively conclude that the presence of TCRM does not invalidate paleointensity studies.

KARL KELLOGG
E. E. LARSON
Department of Geological Sciences, University of Colorado, Boulder 80302
D. E. WATSON
Environmental Science Services Administration Research Laboratories, Geomagnetism Laboratory, Boulder, Colorado 80302

References and Notes

1. J. Verhoogen, *J. Geol.* **70**, No. 2, 168 (1962).
2. K. M. Creer and H. Peterson, *Z. Geophys.* **35**, 501 (1969).
3. M. Ozima and E. Larson, *J. Geophys. Res.* **75**, 1003 (1970).
4. P. J. Wasilewski, *J. Geomagn. Geoelec.* **20**, 129 (1968).
4a. M. Ozima and E. Larson, *ibid.*, p. 337.
5. D. H. Lindsley, *Carnegie Inst. Wash. Year B.* **64**, 144 (1964).
6. T. Nagata and K. Kobayashi, *Nature* **197**, 476 (1963).
7. I. S. E. Carmichael and J. Nicholls, *J. Geophys. Res.* **72**, 4665 (1967).
8. C. S. Grommé, T. L. Wright, D. L. Peck, *ibid.* **74**, 5277 (1969).
9. R. Bruce, *Geophysics* **32**, No. 5, 893 (1967).
10. R. W. Day, W. O'Reilly, S. K. Banerjee, *J. Geophys. Res.* **75**, 375 (1970).
11. E. Thellier and O. Thellier, *Ann. Geophys.* **15**, 285 (1959).
12. Supported in part by grant 1365 from the National Science Foundation.

30 April 1970; revised 10 August 1970

Convection in the Antarctic Ice Sheet Leading to a Surge of the Ice Sheet and Possibly to a New Ice Age

Abstract. *The Antarctic surge theory of Pleistocene glaciation is reexamined in the context of thermal convection theory applied to the Antarctic ice sheet. The ice sheet surges when a water layer at the base of the ice sheet reaches the edge of the ice sheet over broad fronts and has a thickness sufficient to drown the projections from the bed that most strongly hinder basal ice flow. Frictional heat from convection flow promotes basal melting, and, as the ice sheet grows to the continental shelf of Antarctica, a surge of the ice sheet appears likely.*

Wilson (*1*) has suggested that Pleistocene ice ages could be triggered by a surge of the Antarctic ice sheet. He makes the following basic assumptions: (i) the periodicity of the surge is controlled by variations in solar input to the Antarctic ice sheet due to precession of the earth's rotational axis; (ii) a surge begins when the entire ice sheet is underlain by a basal water layer; (iii) the surge creates an ice shelf extending to the Antarctic convergence, causing an increase in the earth's albedo sufficient to preserve the winter snow cover in high latitudes.

Weertman (*2*) gave a quantitative treatment of Wilson's assumption (ii) and concluded that, before a surge could occur, the basal water layer must exceed a "controlling obstacle size" related to bed roughness and the basal shear stress. Once a surge began, however, it could discharge sufficient ice into the Antarctic Ocean to satisfy Wilson's assumption (iii), but as icebergs rather than as a stable ice shelf.

When our estimates of the controlling obstacle size are compared with our estimates of the basal water layer thickness due to gravity sliding and thermal convection, it appears that thermal convection is necessary to make the Antarctic ice sheet surge. The possibility of convection was realized (*3*) when the CRREL core hole drilled to bedrock at Byrd Station, Antarctica (80°1′S,119°31′W), indicated a density inversion 1000 m below the surface (*4*). This density inversion will be confirmed when the compressibility coefficient is definitely established.

An estimate of the controlling obstacle size can be made from the basal sliding velocity U_x'', which is the measured downstream velocity at the surface of the ice sheet, U_x, minus the downstream velocity due to differential motion within the ice, U_x'. On the assumption that laminar flow dominates, U_x' can be estimated from the flow law of ice (*5*):

$$\dot{\gamma} = A(f,T,P)\ \tau^n \qquad (1)$$

where $\dot{\gamma}$ is the effective shear strain rate, τ is the effective shear stress, n is a viscoplastic parameter, and $A(f,T,P)$ is a function of ice fabric f, temperature T, and hydrostatic pressure P. For laminar flow

$$\tau = \tau_{xz} = \rho\ g\ (h - z)\ \tan\theta \qquad (2)$$

where ρ is ice density, g is the acceleration of gravity, θ is the surface slope, x is horizontal and positive downstream, z is vertical with $z = h$ at the surface, and the origin of the orthogonal x,y,z coordinates is placed on the bottom of the ice sheet.

Since $A(f,T,P) = A(z)$, we can combine Eqs. 1 and 2 to obtain

$$U_x' = \int_0^h \dot{\gamma}_{xz}\,dz = \int_0^h A(z)\ \tau_{xz}{}^n\,dz = (\rho\ g \tan\theta)^n \int_0^h A(z)\ (h-z)^n\,dz \qquad (3)$$

where h is the total ice thickness at distance x from the ice divide, and

$$A(z) = A(f,T,P) = B(f)\exp(-Q/RT) = B(f)\exp(-C\ T_M/T) \qquad (4)$$

where Q is the activation energy of self-diffusion, T_M is the pressure melting point, (T/T_M) is the homologous temperature, and C is a constant.

Figure 1 shows the quantitative z dependence of T, (T/T_M), and ρ, and the qualitative z dependence of f at Byrd Station. For a graphical solution of Eq. 3 from Fig. 1:

$$U_x' = \Sigma_h\,\Delta U_x' = \Sigma_z\,\overline{A}\ (\rho\ g \tan\theta)^n\ (h - \bar{z})^n\,\Delta z \qquad (5)$$

where

$$\Delta U_x' = (U_x')_{z_2} - (U_x')_{z_1}$$
$$\overline{A} = \tfrac{1}{2}\,(A_{z_2} + A_{z_1})$$
$$\bar{z} = \tfrac{1}{2}\,(z_2 + z_1)$$
$$\Delta z = z_2 - z_1$$

In zone III of Fig. 1 almost all grains have c axes aligned within 15° of the z axis and the mean temperature is $-20°C$, or $(T/T_M) = 0.93$. Holdsworth and Bull (*6*) found a similar strong single-maximum ice fabric in Meserve Glacier, a polar Alpine glacier in Wright Valley, Antarctica (77°31′S, 162°18′E), and from deformation studies they obtained $n = 1.6$ and $A = 4.8 \times 10^{-9}$ bar^{-n} sec^{-1} at a temperature of $-18°C$, or $(T/T_M) = 0.935$. Higashi, Koinuma, and Mae (*7*) measured the bending creep of single ice crystals oriented for easy glide. They observed $n = 1.6$ and $Q = 15.8$ kcal mole^{-1} between $-4.8°C$ and $-40.0°C$. These values of n, Q, and A are used at Byrd Station, where $\tan \theta = 2 \times 10^{-3}$, to give $B(f) = 1.8 \times 10^5$ bar^{-n} sec^{-1} and $U_x' = 9$ m per year for zone III, using Eqs. 4 and 5. Similarly, the fabric, temperature, and thickness of the other zones leads to an estimate of $U_x' = 12$ m per year at Byrd Station.

At Byrd Station, $U_x = 22$ m per year, as calculated from deformation rates of the U.S. Geological Survey surface strain network extending along a flow line to the ice divide 160 km northeast of Byrd Station (*8*). Hence $U_x'' = U_x - U_x' = 10$ m per year is the estimated basal sliding velocity at Byrd Station.

According to the theory of glacier sliding (*9*),

$$U_x'' = K \frac{\tau_s}{L_c} \left(\frac{L_i'}{L_i} \right)^2 = K^* \, r^{n+1} \, \tau^{(n+1)/2} \quad (6)$$

where K and K^* are constants, τ_s is the basal shear stress, L_c is the controlling obstacle size, L_i' is the average distance between obstacles of average dimension $L_i = (L_x \; L_y \; L_z)_i^{1/3}$, and $r = (L_i'/L_i)$ is the bed roughness factor, where r is constant for all obstacle sizes. We have used $n = 1.6$ in estimating U_x''. Weertman prefers $n = 3$, since this value is a fair average of the range $1 \leqslant n \leqslant 4.5$ predicted theoretically and observed experimentally. Table 1 lists values of L_c and r obtained from Eq. 6 for both $n = 1.6$ and $n = 3$, by the use of $U_x'' = 10$ m per year and $\tau_s = 0.39$ bar at Byrd Station. Cavitation behind obstacles is possible for $n = 1.6$ but unlikely for $n = 3$. We will take $L_c \approx 2$ cm.

A surge of the Antarctic ice sheet occurs when $L_c \leqslant L_w$, where L_w is the thickness of the basal water layer. According to Weertman (*2*),

$$L_w = [(12 \, \eta_w \, V_x)/(\rho \, g \tan \theta)]^{1/3} \quad (7)$$

where η_w is the coefficient of viscosity of water and V_x is the volume of water moving downstream per unit time per unit distance. If H_G is the geothermal heat flow, H_F is the frictional heat generated by differential motion within the ice sheet, and H_M is the latent heat of melting,

$$V_x = \int_0^x [(H_G + H_F)/H_M] \, dx \quad (8)$$

If it is assumed that only gravity sliding contributes to H_F,

$$V_x = \int_0^x [H_G + (U_x' + U_x'') \, \tau_s/J] H_M^{-1} \, dx \quad (9)$$

where J is the mechanical equivalent of heat. For an average annual snow accumulation rate, a,

$$(U_x' + U_x'') \, \tau_s = a x \rho g \tan \theta \quad (10)$$

When $x = 160$ km along the flow line from the ice divide to Byrd Station, average values are $\bar{a} = 16.4$ g cm^{-2} per year, $\bar{\theta} = 1.8 \times 10^{-3}$, $\bar{h} = 2700$ m, and $\bar{U}_x = 10$ m per year (*10*), which gives $L_w = 0.166$ cm. Hence, $L_c = 12 \; L_w$ for $L_c = 2$ cm, and gravity sliding seems incapable of producing a surge of the Antarctic ice sheet.

I have applied the theory of thermal convection to the Antarctic ice sheet and concluded that convection is presently possible (*3*). The steep shear zones shown in Fig. 2 may be convection plumes. The Rayleigh number is taken as:

$$Ra = \rho g \alpha \, \beta \, d^4 \, \kappa^{-1} \, n \, B(f) \, \tau_c^{n-1} \exp(-CT_M/T) \quad (11)$$

where α is the coefficient of thermal expansion, β is the superadiabatic temperature gradient through ice thickness, d, below the density inversion, κ is the thermometric diffusivity, τ_c is the buoyancy effective shear stress driving convection, (T/T_M) is for the basal ice, and $Ra^* = 7 \times 10^4$ is the critical Rayleigh number near the center of the Antarctic ice sheet.

Once thermal convection begins, it will tend to develop an ice fabric favorable for convection flow and $B(f)$ will be reduced two or three orders of magnitude to approximately the single crys-

Table 1. Controlling obstacle sizes (L_c) estimated for the Antarctic ice sheet with the data from Byrd Station. At Byrd Station:

$h = 2164$ m. $\quad \tau_s = \rho \; g \; h \tan \theta = 0.39$ bar.

$\tan \theta = 2 \times 10^{-3}$. $\quad P = \rho \; g \; h = 195$ bars.

$U_x \approx 10$ m yr^{-1}.

For cavitation: $(P/\tau_s) = 500 \leqslant (r^2/k) \sin^2 \phi$. The symbol ϕ indicates the angle between the maximum slope of an obstacle and the average slope of the bed; $\phi = 30°$ (below) is an assumption.

Constants	Cavitation		No cavitation	
	$n = 1.6$	$n = 3$	$n = 1.6$	$n = 3$
ϕ	30°	30°	30°	30°
k	0.858	2.314	0.858	2.314
$(r^2/k) \sin^2 \phi$	403	196	488	268
K (cm^2 yr^{-1} bar^{-1})	36.8	13.7	36.8	13.7
K^* (cm yr^{-1} bar$^{-(n+1)/2}$)	5.65	0.194	3.24	0.0685
r	11.75	13.5	14.45	17.6
L_c (cm)	2	1	3	1.66

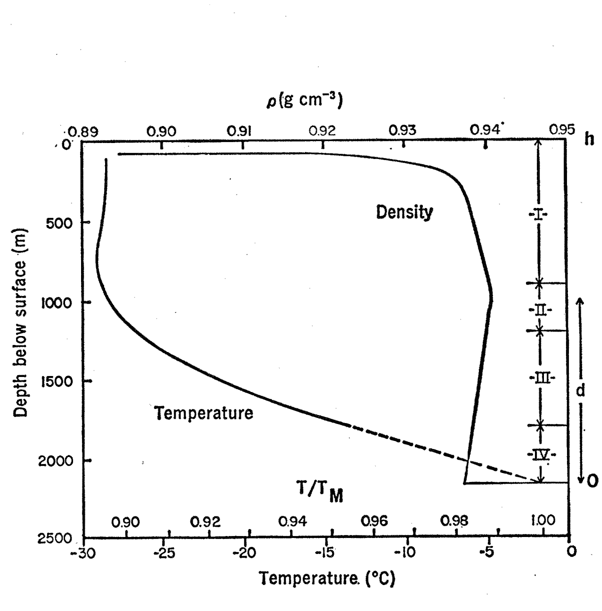

Fig. 1. Variation of density (ρ), temperature (T), and ice fabric with depth through the Antarctic ice sheet at Byrd Station (*4*). Zone I: randomly oriented fabric, grain size increasing with depth. Zone II: transition from random to single-maximum fabric, grain size decreasing with depth. Zone III: strong single-maximum fabric with near-vertical c axes, fine grain size, and numerous horizontal "shear bands" with very fine grain size. Zone IV: weak multiple-maximum fabric, very coarse intergrown grains.

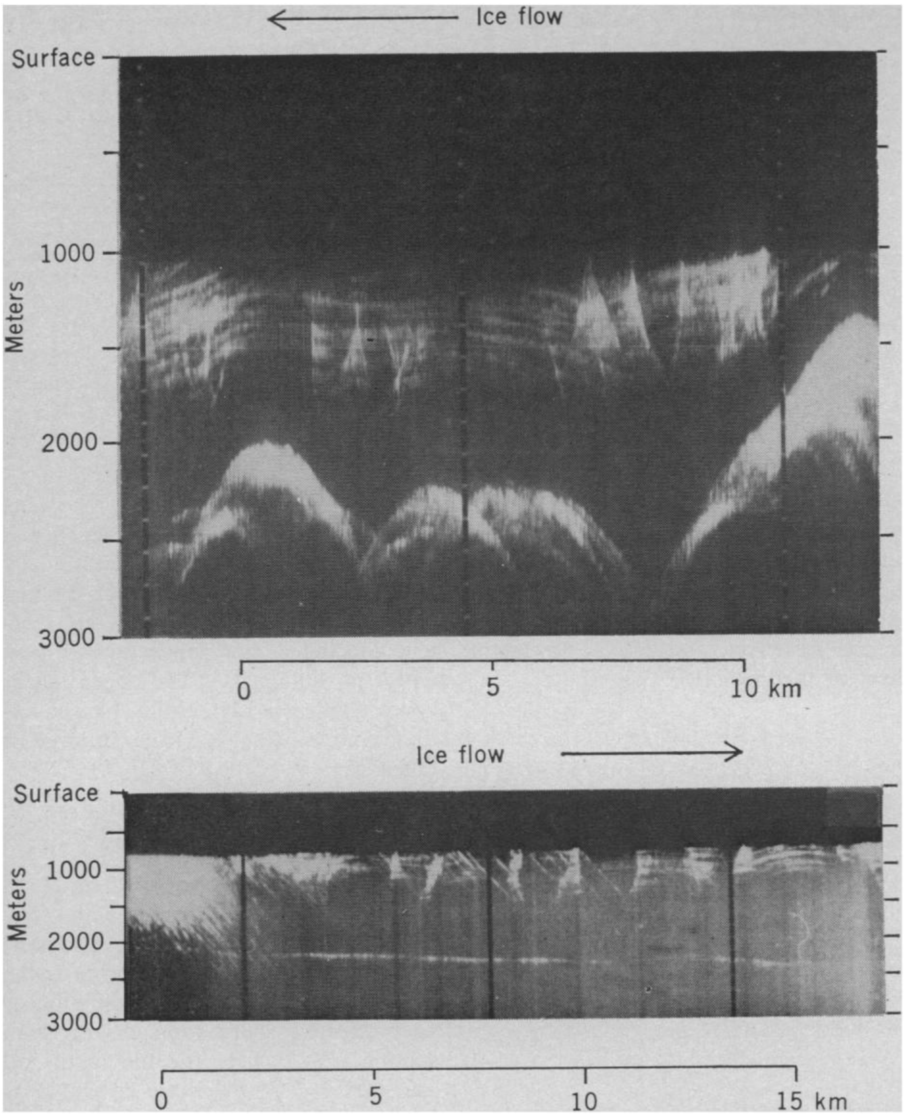

Fig. 2. Subglacial profile over the Gamburtsev Mountains (top) and Marie Byrd Land (bottom) revealed by radio echo exploration of the Antarctic ice sheet. The near-vertical deep shear planes in ice overlying both rough and smooth bedrock topography suggest vertical flow unrelated to bed topography, and they may be convection plumes. [Photographs supplied by Dr. G. deQ. Robin and the Scott Polar Research Institute, Cambridge, United Kingdom]

tal value. Hence, for fully developed convection flow $Ra \gg Ra^*$, and the horizontal velocity of basal convection flow is approximately (*11*):

$$U_x''' = K_x \, Ra^{2/3} \, \kappa/d \qquad (12)$$

where $K_x = 0.141$ and where flow converging on ascending convection plumes is restricted to a narrow layer above the base of the ice sheet. Equation 8 now becomes

$$V_x = \int_0^x [H_G + (U_x' + U_x'')\,\tau_s/J + U_x'''\,\tau_c/J] H_M^{-1}\,dx \qquad (13)$$

Since β is fairly constant through d, we can approximate τ_c by (*3*):

$$\tau_c = \sigma_c/\sqrt{3} = -(1/2\sqrt{3})\,\rho_0\, g\, \alpha\, d\, \Delta T \qquad (14)$$

where σ_c is the vertical buoyancy stress, ρ_0 is the maximum ice density, and ΔT is the temperature change through d.

Fully developed thermal convection is theoretically capable of attaining flow velocities that overwhelm flow velocities due to gravity sliding. Hence, the frictional heat due to convection flow will dominate the other heat sources, and we can write

$$V_x \approx \int_0^x \frac{U_x'''\,\tau_c}{H_M\,J}\,dx = \frac{\Sigma_x \bar{U}_x'''\,\bar{\tau}_c\,\Delta x}{H_M J} \qquad (15)$$

Equation 15 can be evaluated by employing Nye's (*12*) formula for the equilibrium profile of an ice sheet above a flat, horizontal bed:

$$\left(\frac{h^*}{H^*}\right)^{(2n+4)/(n+1)} + \left(\frac{x^*}{X^*}\right)^{(n+3)/(n+1)} = 1 \qquad (16)$$

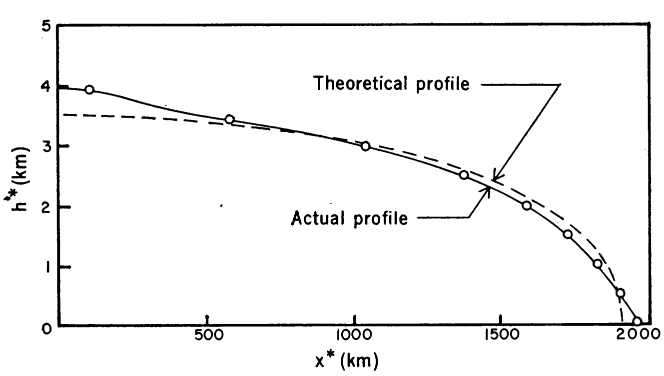

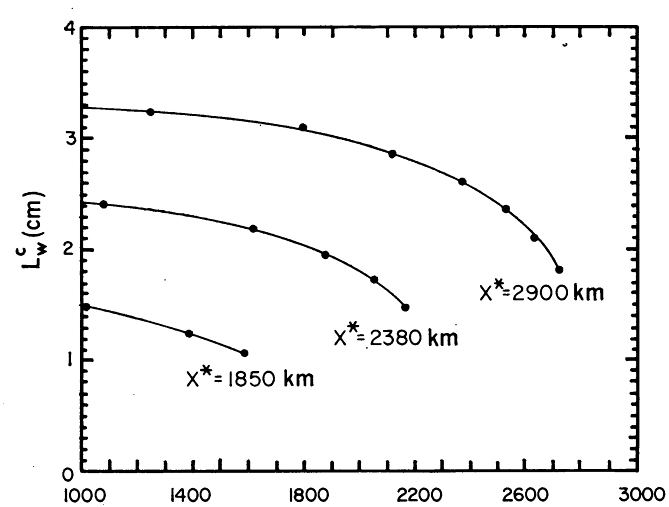

Fig. 3 (left). An actual profile of the Antarctic ice sheet compared with a theoretical profile obtained by using Eq. 16 and $n = 1.6$ (*13*). The abnormally high h^* at $x^* = 100$ km is due to the subglacial Gumburtsev Mountains. Fig. 4 (right). The variation of basal water layer thickness due to thermal convection (L_w^c) with distance from the center of the idealized Antarctic ice sheet (x^*) for various ice sheet radii (X^*). Beyond the end of the curves the ice sheet is too thin for thermal convection. The total basal water layer thickness is $L_w = L_w^c = L_w^s$, where L_w^s is due to gravity sliding and geothermal heat, increases with x^*, and becomes dominant as $x^* \rightarrow X^*$.

where h^* and x^* are vertical and horizontal coordinates, respectively, of the surface of the ice sheet with respect to an origin at the center of the ice sheet and at set level; and H^* and X^* are the maximum values, respectively, of h^* and x^*. Figure 3 shows that Eq. 16 gives a first-order fit to the Antarctic ice sheet for $n = 1.6$. Shumsky (*13*) argues that the unglaciated elevation of Antarctica averaged about 0.5 km above sea level. Weertman (*14*) shows that the ice sheet will isostatically depress the bed to about one-third of the ice thickness, so that $h = 1.5$ ($h^* -$ 0.5 km), where ($h^* - 0.5$ km) is the ice thickness above the unglaciated bed. Assuming that the density inversion occurs 1 km below the firn surface, as in Fig. 1, the buoyancy stress will act through ice of thickness $d = [1.5\ (h^* -$ 0.5 km)] $-$ 1 km. The surface slope of the ice sheet is:

$$\tan\theta = \frac{dh^*}{dx} = -\frac{n+3}{2n+4}\left(\frac{H^*}{X^*}\right)\frac{\left(\frac{x^*}{X^*}\right)^{(n+3)/(n+1)}}{\left(\frac{h^*}{H^*}\right)^{(2n+4)/(n+1)}} \qquad (17)$$

We can now calculate L_w for various values of x^* and X^* by solving Eqs. 7 through 17 with $n = 1.6$, $C = 29.1$, and $B(f) = 1.38 \times 10^7$ bar^{-n} sec^{-1} obtained from the data of Higashi, Koinuma, and Mae (*7*), $\beta = 10^{-4}$ °C cm^{-1} obtained from theoretical temperature gradients in polar ice sheets (*15*), $d = 1.5\ h^* - 1.75$ km, $\rho = 0.92$ g cm^{-3}, $g = 980$ cm sec^{-2}, $\alpha = 15.3 \times 10^{-5}$ °C^{-1}, $\kappa = 1.18 \times 10^{-2}$ cm^2 sec^{-1}, $\eta_w = 1.8 \times 10^{-2}$ poise, $H_M =$ 80 cal g^{-1}, and $J = 4.19 \times 10^7$ dynes cm^{-1} cal^{-1}. The results are shown in Fig. 4. According to Weertman's theory, a surge will not begin until $L_c \leqslant L_w$ at all values of x^*, and Fig. 4 shows that for $L_c \approx 2$ cm this condition is not approached until $X^* \approx 2900$ km. An ice sheet of this radius would extend to the continental shelf of Antarctica.

The principal assumptions we have made concern (i) the density inversion as a general feature of the Antarctic ice sheet, (ii) the estimation of basal sliding velocities from the Byrd Station core hole and the U.S. Geological Survey strain network data, (iii) the applicability of convection theory derived for a viscous fluid to a viscoplastic solid, and (iv) the equilibrium profile of the Antarctic ice sheet. If the assumptions made are valid, the Antarctic ice sheet will surge when the ice sheet approaches the continental shelf of Antarctica. Presumably the surge will begin when the critical thickness of the basal water layer extends to the edge of the ice sheet along one or more fronts. These fronts will then surge, causing a slumped region to proceed inland from each front until the entire ice sheet has collapsed to the postsurge equilibrium thickness.

Weertman's surge theory, modified to include the frictional heat of thermal convection, should apply to both polar ice sheets and Alpine glaciers. The basal water layer thickness is a function of the surface slope and the frictional heat generated by ice flow. Although no frictional heat from convection flow is possible for surging Alpine glaciers, their surface slopes are orders of magnitude greater than surface slopes of the Antarctic ice sheet (*16*).

Strong evidence suggests that the Antarctic ice sheet may have been more extensive in the past (*17*). However, it is not known whether the present equilibrium profile of the ice sheet was maintained during these past advances. If not, these advances may themselves have been surges, which suggests that our estimate of the controlling obstacle size is too large (*18*). Also, at present the Antarctic ice sheet probably does not behave dynamically as a unit, and possibly various sectors could surge independently. However, the larger the ice sheet becomes, the more it should behave as a unit, and, if it extended to the continental shelf, presumably it could be dynamically treated as such.

T. Hughes

Institute of Polar Studies and Department of Civil Engineering, Ohio State University, Columbus 43210

References and Notes

1. A. T. Wilson, *Nature* **201**, 147 (1964); *ibid.* **210**, 477 (1966); *Can. J. Earth Sci.* **6**, 911 (1969).
2. J. Weertman, *J. Glaciol.* **6**, 191 (1966).
3. T. Hughes, paper presented at the 21st Alaska Science Conference (University of Alaska, 16–19 August 1970). The paper presented was an application to polar ice sheets of the convection theory by G. Schubert, D. L. Turcotte, and E. R. Oxburgh [*Geophys. J. Roy. Astron. Soc.* **18**, 441 (1969)].
4. CRREL: U.S. Army Cold Regions Research and Engineering Laboratory. For data from core hole, see A. J. Gow, H. T. Ueda, D. E. Garfield, *Science* **161**, 1011 (1968); A. J. Gow, *Int. Ass. Sci. Hydrol. Publ.* **86**, 78 (1970).
5. For a review of experimental flow laws, see L. Lliboutry, *Int. Ass. Sci. Hydrol. Publ.* **86**, 216 (1970). For a review of theoretical flow laws, see J. Weertman, *Trans. Amer. Soc. Metals* **61**, 681 (1968).
6. G. Holdsworth and C. Bull, *Int. Ass. Sci. Hydrol. Publ.* **86**, 204 (1970).
7. A. Higashi, S. Koinuma, S. Mae, *Jap. J. Appl. Phys.* **4**, 575 (1965).
8. The surface velocity was calculated by I. Whillans (Ohio State University, Institute of Polar Studies).
9. J. Weertman, *J. Glaciol.* **5**, 287 (1964).
10. Average values were obtained from the following sources: $\bar{a}$, H. Brecher, unpublished data (Ohio State University, Institute of Polar Studies); $\bar{\theta}$, W. H. Chapman, thesis, Ohio State University (1966); $\bar{h}$, G. Dewart, *Antarctic J.* **3**, 114 (1968); $\bar{U}_x$, I. Whillans, unpublished data (Ohio State University, Institute of Polar Studies).
11. D. L. Turcotte and E. R. Oxburgh, *J. Fluid Mech.* **28**, 29 (1967).
12. J. F. Nye, *J. Glaciol.* **3**, 493 (1959).
13. P. A. Shumsky, *Int. Ass. Sci. Hydrol. Publ.* **86**, 327 (1970).
14. J Weertman, *J. Glaciol.* **3**, 953 (1961).
15. G. DeQ. Robin, *ibid.* **2**, 523 (1955); U. Radok, D. Jenssen, W. Budd, *Int. Ass. Sci. Hydrol. Publ.* **86**, 151 (1970).
16. M. F. Meier and A. S. Post, *Can. J. Earth Sci.* **6**, 807 (1969); A. S. Post, *J. Glaciol.* **8**, 229 (1969). Papers presented at the Seminar on the Causes and Mechanisms of Glacier Surges (St. Hilaire, Quebec, 10–11 September 1968) and the Symposium on Surging Glaciers (Banff, Alberta, 6–8 June 1968) are published in *Can. J. Earth Sci.* **6**, No. 4, part 2 (August 1969).
17. J. T. Hollin, *J. Glaciol.* **4**, 172 (1962); C. Bull, *ibid.*, p. 240; J. H. Mercer, *Geol. Soc. Amer. Bull.* **79**, 771 (1968).
18. J. Weertman, *Can. J. Earth Sci.* **6**, 929 (1969).

19. Contribution No. 170 of the Institute of Polar Studies.

13 August 1970

Radioreceptor Assay of Adrenocorticotropic Hormone: New Approach to Assay of Polypeptide Hormones in Plasma

Abstract. *Biologically active iodine-125–labeled adrenocorticotropic hormone (ACTH) binds specifically to ACTH receptors extracted from adrenals. Unlabeled ACTH at 1 picogram per milliliter significantly displaces labeled ACTH from these receptors. This system, which appears to be applicable to all polypeptide hormones, provides a rapid and sensitive method for measurements of biologically active ACTH in dilute whole plasma.*

Since its original application to the measurement of plasma insulin (*1*), radioimmunoassay has been used for the assay of many polypeptide hormones. In addition to the specificity and great sensitivity obtainable by the use of carefully selected antiserums to hormones, this method readily allows precise measurement of hormone concentrations on a large number of specimens. Disadvantages have been that the basis for specificity is immunological